INL/CON-15-36462
PREPRINT

Impact of Modifications in Continuous Recycling System for U/Pu and U/TRU with Fast and Thermal Reactors on Fuel-cycle Performance and Waste Characterization

Physics of Reactors Conference (PHYSOR 2016)

Hikaru Hiruta, Gilles J. Youinou, Brent W. Dixon

May 2016

The INL is a
U.S. Department of Energy
National Laboratory
operated by
Battelle Energy Alliance

IMPACT OF MODIFICATIONS IN CONTINUOUS RECYCLING SYSTEM FOR U/PU AND U/TRU WITH FAST AND THERMAL REACTORS ON FUEL-CYCLE PERFORMANCE AND WASTE CHARACTERIZATION

Hikaru Hiruta, Gilles J. Youinou, and Brent W. Dixon
Nuclear Systems Design and Analysis Division
Idaho National Laboratory, Idaho Falls, Idaho, USA
hikaru.hiruta@inl.gov
gilles.youinou@inl.gov
brent.dixon@inl.gov

ABSTRACT

This paper studies the impact of modifications in continuous U/Pu and U/TRU recycling systems on fuel-cycle performance and waste characterization. The continuous recycling systems considered in this paper are multi-stage scenarios consisting of sodium-cooled fast reactors (SFR) and mixed-oxide (MOX) fueled pressurized water reactors (PWR). The study was performed by introducing a series of fuel-cycle cases that slightly differ in their fuel-cycle scenarios, core designs, and types of heavy metals (HM) recycled (Pu or TRU). The major exchange in the fuel-cycle scenarios considered here occurs in the PWR-MOX stage such that one set of cases recycles its discharged Pu/TRU and fabricate MOX fuel by topping Pu/TRU recovered from SFR blankets, and the other uses only recovered Pu/TRU from SFR blankets, and its discharged Pu/TRU is sent to SFR metallic fuel fabrication. All analyses performed in this paper also take into account 1% of annual growth in electric power production. Therefore, the design of reactor cores and fuel-cycle systems must be able to produce additional Pu/TRU in order to cover additional reactors built for the 1% growth in each year.

Key Words: **Sodium-cooled Fast Reactor, Pressurized Water Reactor, U/Pu & U/TRU Recycling, MOX, Fuel-Cycle Performance, Waste Characterization**

1. INTRODUCTION

The multi-recycling of plutonium/transuranics (Pu/TRU) from the system consisting of both sodium-cooled fast reactors (SFR) and mixed-oxide (MOX) fueled Pressurized Water Reactors (PWR) is considered as one of the promising fuel-cycle options that could potentially reduce the amount of high-level waste (HLW) and uranium disposal while improving the uranium utilization compared to the current U.S. fuel-cycle [1,2]. The SFR design considered in these groups must have a sufficiently large Pu/TRU conversion rate so that PWR-MOX operation can be supported by extra Pu or TRU produced by the SFR blanket.

The fuel-cycles of this type are sometimes categorized to either Pu-only or TRU recycling. The former recycles only U/Pu from the discharged fuel and most of minor actinides (MA) and fission products (FP) are sent to waste disposal. The latter also recycles MAs, therefore the majority of

disposed waste consists of FPs resulting in less toxic to the environment compared to that from Pu-only recycling. For the multistage recycling systems such as the one mentioned above, there could be some options to reduce the MA content in the disposed waste from Pu-only recycling by modifying the recycling paths even without introducing additional systems. For instance, there could be some impacts on waste characteristics if the PWR-MOX stage is switched from a system using the fuel consisting only of Pu/TRU from the SFR blanket to one that also includes recycling of discharged Pu/TRU in the PWR-MOX fuel back to the PWR. The latter substantially increases the Pu enrichment of MOX fuel, which could affect the design of the SFR in order to support the PWR-MOX system.

In this paper, the impact of modifications in closed fuel-cycle scenarios consisting of SFR and PWR-MOX systems on SFR core design, mass-flow and waste characterization will be investigated. The study will be performed by introducing a series of fuel-cycle cases that slightly differ in their fuel-cycle scenarios, core designs, and type of heavy metals (HM) recycled (Pu or TRU). All analyses performed in this paper also take into account 1% of annual growth in electric power production. Therefore, the design of reactor cores and fuel-cycle systems must be able to produce additional Pu/TRU in order to cover additional reactors built for the 1% growth in each year.

2. MODELS AND PROBLEM DESCRIPTIONS

2.1. Descriptions of Computational Tools Used for Reactor Core Modeling

The SFR stage fuel-cycle analyses coupled with whole core reactor physics calculations are performed with the fuel-cycle analysis code REBUS-3 [4]. Its neutronics solver DIF3D-8 [5] can solve 1-, 2- and 3-D multigroup steady-state neutron diffusion equations in Cartesian or hexagonal geometries via nodal approximation. Utilizing the flux/power distribution from DIF-3D calculations, REBUS-3 can perform transmutation of reactor fuel and calculate mass flow between reactors and reprocessing plants based on the user specified fuel management path and criteria. The hexagonal-z geometry option is used for modeling 3D sodium-cooled fast reactor (SFR) cores by applying the periodic boundary condition in the radial plane in order to represent a one third core rotational symmetry. Table 1 summarizes the dimensional parameters, and Figure 1 shows the radial layout of the full-core model. The radial core configuration is based on the S-PRISM design with metallic driver and blanket fuels [3] but includes extra radial blanket zones (2+ extra rows of outer core radial blanket assemblies and ones in place of Gas Expansion Modules (GEM)). In this paper, cores having both long and short cycle lengths will be examined. For the core with long cycle length, the residence time of driver and inner blanket assemblies is set to 3 cycles (3 × 547.875 EFPD) whereas that of outer blanket assemblies is set to 5 cycles in order to enhance the Pu breeding. On the other hand, the residence time of all driver and blanket assemblies in the core with short cycle length is set to 5 cycles (5 × 365.25 EFPD). No driver or blanket assembly shuffling is considered in this model while the original S-PRISM design in Reference 3 performs blanket shuffling. The axial zone is subdivided into a total of 30 nodes. The active fuel zone has a total of 10 axial nodes, in which sizes vary from 4.5 cm to 10.7 cm. The reference model has 40 cm of axial blanket. The equilibrium cycle condition is searched by adjusting Pu/TRU enrichment so that the core can maintain critical throughout the specified cycle length. It is important to note that for the fast reactor design the peak discharge fast fluence should not exceed the limit of HT-9 cladding (4×10^{23} n/cm^2). A set of mul-

tigroup cross sections for the nodal diffusion calculations is obtained with the MC^2-3 code [6] using ENDF/B-VII.0 data. MC^2-3 solves the consistent multigroup P_1 equation using ENDF/B type data to calculate fundamental mode spectra for generating multigroup cross sections in the specified energy group structure (33 groups). For the preparation of self-shielded cross sections, the numerical integration of pointwise cross sections is performed within the resolved resonance range, whereas the analytic resonance integral method is used for the unresolved resonance range. Although a one-dimensional unit-cell calculation capability is available in MC^2-3 for taking into account the spatial heterogeneity effect, the homogeneous medium option has been chosen for this application since the pin-wise heterogeneity effect is not important for the SFR core modeling. The beginning of equilibrium cycle (BOEC) fuel compositions and structural material compositions are used as input parameters for MC^2-3 calculations.

Table 1. Reference SFR fuel and dimensional specifications.

Parameter	Driver	Blanket
Fuel metal alloy	U-Pu/TRU-10Zr	U-10Zr
Duct and cladding material	HT-9	HT-9
Coolant material	Na	Na
Fuel temperature [°K]	850.0	850.0
Structural material temperature [°K]	750.0	750.0
Coolant temperature [°K]	713.7	713.7
Assembly pitch [cm]	16.2379	16.2379
Fuel height [cm]	147.3 (Active fuel height = 107.3)	
Number of assemblies	138	49 (Inner), 180 (Outer)
Fuel volume fraction [%]	26.5	41.8

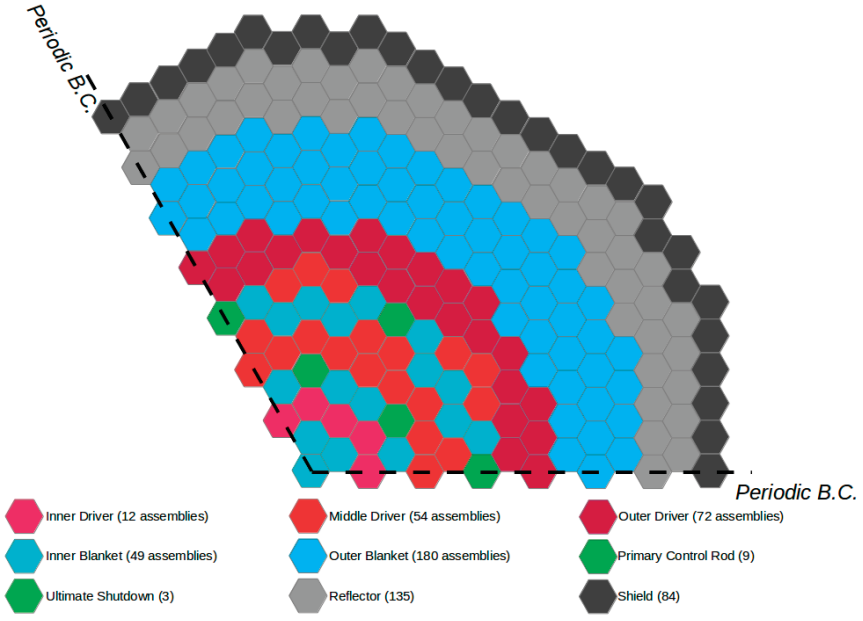

Figure 1. SFR core model radial layout.

The PWR fuel-cycle stage is approximated by burnup calculations of a quarter 17×17 assembly model using the TRITON module in SCALE 6.1.3 [7]. NEWT, which is the 2D discrete ordinates transport solver in non-orthogonal geometries, has a capability to model heterogeneous assembly geometry by closely approximating curved geometries. The TRITON module, which effectively couples NEWT with the ORIGEN-S depletion module, performs burnup calculations together with the automated cross section processing such as resonance self-shielding calculations by BONAMI (unresolved range) and CENTRM (resolved range) at each depletion sub-interval. The 238-group ENDF/B-VII.1 library in SCALE 6.1.3 is used for these calculations. The assembly dimensions and some of physical data are presented in Table 2. Figure 2 shows the plot of modeled assembly geometry. Each pin-cell zone of the sub-assembly model is subdivided into 4×4 equivalent cells. The color of each fuel-pin cell represents the burnup zoning. The Coarse-Mesh Finite Difference (CMFD) acceleration method is applied by setting each unit pin-cell as a coarse-mesh for low-order equations in order to accelerate the convergence of inner iterations. The order of scattering is set as P_3 for the moderator and P_1 for other regions. The product quadrature set is assigned to have six directions per quadrant (2 polar × 3 azimuthal angles). For depletion calculations, 230 nuclides are included in trace quantities by using *addnux=3* in order to accurately estimate the nuclide impacts on cross section processing through the end of cycle (EOC).

The 3-batch fuel management scheme is assumed for PWR-MOX burnup calculations. The core average specific power is set to 35.36 W/g. Then each assembly can reach an average discharge burnup of 50 GWd/t in 1414 EFPD (3 cycles). Since the full-core calculation is not performed for the PWR fuel-cycle stage, the initial core inventory necessary for the mass-flow calculation is estimated by summing compositions at the beginning of the equilibrium cycle (BOEC), 1/3×1414 EFPD, and 2/3×1414 EFPD and normalizing to the mass of heavy-metals in a 1.1 GWe PWR core which requires approximately 90 metric tons of oxide fuel [8].

Table 2. Reference PWR assembly fuel and dimensional specifications.

Parameter	Type/Value
Fuel material	MOX
Cladding material	Zircaloy-4
Fuel density [g/cm^3]	10.0
Number of fuel pins/assembly	264
Inner pin diameter [cm]	0.81916
Outer pin diameter [cm]	0.94996
Gap size [cm]	0.00825
Fuel pin-pitch [cm]	1.25984
Average fuel temperature [°K]	900
Gap temperature [°K]	750
Clad temperature [°K]	629
Moderator temperature [°K]	580

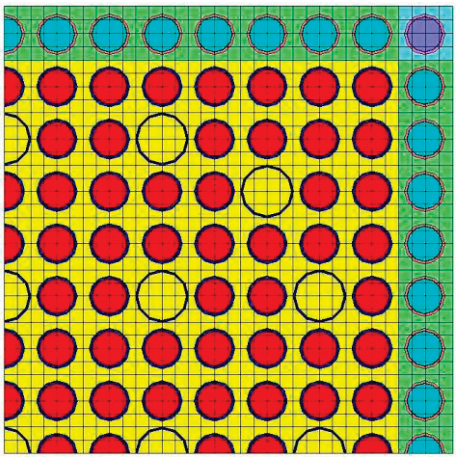

Figure 2. A quarter 17×17 PWR assembly model.

For the estimation of radiological data in waste characterization, it is important to accurately generate the post-irradiated isotopic information. Since the PWR fuel-cycle stage is approximated by a subassembly model, the same simulation suite (i.e., SCALE 6.1.3) is used to directly transfer the post-irradiated isotopic composition into its depletion module ORIGEN-S [9] to perform nuclide decay calculations. For the SFR fuel-cycle stage, depletion calculations of each zone (driver, axial, inner, and outer blanket) by ORIGEN-2.2 [10] are performed over the residence time of each zone with zone-wise specific powers calculated by means of solutions from REBUS-3 full-core calculations. The region-wise one-group cross sections of each actinide are generated by collapsing 33-group fission, (n,γ), and (n,2n) cross sections from the ISOTXS file by group-flux integrals obtained by REBUS-3 calculations and then fed into ORIGEN-2.2 depletion calculations. After depletion calculations of each zone, fission product compositions are extracted and their total mass is normalized to the discharged lumped fission product mass from REBUS-3 full-core calculations. Utilizing resulting fission product compositions along with discharged actinide compositions from REBUS-3 calculations, new ORIGEN-2.2 calculations are performed in the decay mode over time spans of 5 years after discharge for SNF, an additional 2 years for separated recovered uranium (RU) and Pu/TRU, and 10^6 years for the nuclear waste that contains all of fission products and some of the actinides separated or lost during the reprocessing.

All calculated radiological data are normalized to the unit per energy generation in GWe-EFPY by imposing the power sharing ratio between SFRs and PWRs (70% SFRs - 30 % PWRs). The ingestion and inhalation radiotoxicities are estimated by multiplying calculated radioactivity by effective dose coefficients (in the unit of Sv/Bq) obtained from the most recent publication of the International Commission of Radiological Protection (ICRP) [11].

2.3. Mass-Flow Calculations

The closed fuel-cycle scenarios analyzed in this report consist of two stages, a SFR fuel-cycle stage and a PWR fuel-cycle stage. The power-sharing ratio between SFRs and PWRs in this study is fixed to 70% - 30%. Both Pu-only and TRU recycling systems are analyzed. Two types of fuel cycle scenarios are considered, for which mass-flow diagrams are shown in Figure 3. In the Type-a scenario,

the natural uranium (NU), recovered uranium (RU) and Pu/TRU from Stage 1 (SFR with CR > 1.0) are used to make TRU/Pu-U metallic fuel for the SFR. The metallic driver fuel is irradiated to a burnup of ~100 GWd/t in the SFR breeder with a high Pu/TRU conversion ratio (~1.5). The SFR axial blanket goes to the same reprocessing path as that of the driver fuel. The mixed oxide (MOX) PWR fuel is irradiated to a burnup of 50 GWd/t. Pu/TRU discharged from the PWR is recycled and topped with some of the recovered Pu/TRU from the SFR blanket in Stage 1 in order to cast new PWR-MOX fuel. The SFR driver fuel is fabricated from Pu/TRU recycled from its driver and blanket fuels. The Type-b scenario also consists of two stages with similar size of reactors. However, only the recovered Pu/TRU from the blanket is used to fabricate MOX fuel for Stage 2. In the Type-b scenario, recovered Pu/TRU and RU from Stage 2, recovered Pu/TRU and RU from the driver of Stage 1, and depending on the case some portions of Stage 1 blanket Pu/TRU are used to make Stage 1 driver metallic fuel. In both scenarios, discharged fuel is stored for 5 years and then reprocessed in 2 years. Fission products (FPs) and minor actinides (MA) from both stages are stored and then sent to a disposal site.

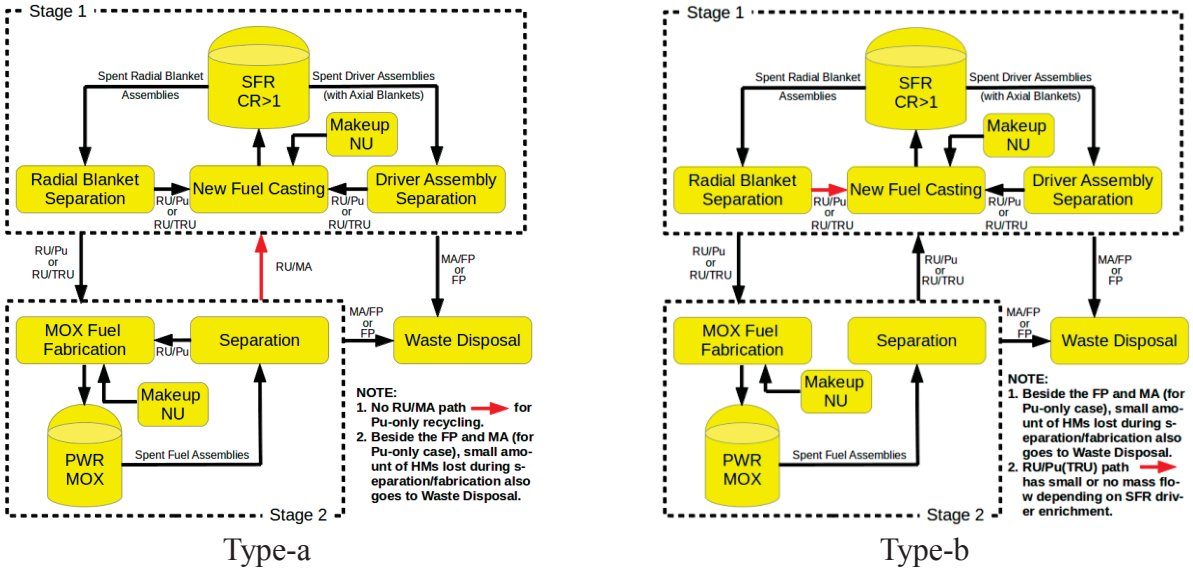

Figure 3. Mass-flow diagrams for Type-a and Type-b scenarios.

There are tight interactions of mass-flow between the SFR and PWR in the Type-b scenario. This is one of major differences from the Type-a scenario, in which only excess amount of Pu/TRU from the SFR blanket is sent to the PWR, and the recovered fuel is recycled back to the same stage. (Note that the TRU recycling in Type-a separates PWR MAs and uses them for SFR driver fuel.) Since the PWR-MOX fuel in Type-b is fabricated only using the material from the SFR blanket fuel, it has significantly high fissile quality (~95 wt%). This will result in significantly lower TRU content in the PWR fuel compared to Type-a (from 9.1 wt% to 4.1 wt%) and thus reduce the MA content in the discharged fuel. However, the fissile quality of the fresh SFR driver fuel in Type-b will be lowered compared to that in Type-a because it is mainly fabricated using recovered Pu/TRU from the SFR driver and PWR-MOX. As a result, Pu/TRU content in the SFR fuel increases along with MA content in the discharged fuel. These changes may have some positive or negative impacts on the core design, as well as results of the waste characterization. Because of mass-flow interactions be-

tween the two stages in the Type-b scenario, the calculation involves an iterative procedure. The 70/30 SFR/PWR power sharing ratio allows the fresh PWR-MOX fuel to be fabricated using 100% Pu/TRU recovered from the SFR blanket.

All analyses in this study assume 1% annual growth of electric power production by fixing the power-sharing ratio of the two-stage fuel-cycle scenario as 70 % SFRs – 30 % PWRs. A simple mathematical expression is derived in order to simulate the dynamically evolving equilibrium condition for reactor core models in the two-stage fuel-cycle scenario considering 1% of annual growth. The unused amount of Pu/TRU at year n, U_n, can be calculated by:

$$U_n = dm_n - \sum_{i=1}^{2}\left(f_i \cdot dm_{i,n}^{C} + F_i \cdot dM_{i,n}\right) \text{ [t]}, \quad (1)$$

where dm_n, $dm_{i,n}^{C}$, $dM_{i,n}$, f_i and F_i refer to the excess amount of Pu/TRU, charged amount of Pu/TRU for additional fleets at each stage, BOEC Pu/TRU inventory for additional fleets at each stage, ratio of fissile content in charged fuel, and BOEC core inventory of Stage i with respect to that of the excess Pu/TRU. The SFR core design is determined so that the value U_n turns out to be close to zero every year. Although the equation given above does not predict the equilibrium condition exactly since the ratio of fissile content is introduced for the quick estimation of Pu/TRU inventory of additional fleets, it will provide the approximate size of the SFR core needed to support 1% annual growth.

3. RESULTS AND DISCUSSIONS

In all analyses in this section, the power-sharing ratio of the two-stage fuel-cycle scenario is set to 70 % SFRs – 30 % PWRs, and thermal efficiencies of the SFR and PWR are 40 % and 33 %, respectively. For the mass-flow calculations, total of 1.2 % reprocessing loss is taken into account (1.0 % separation loss and 0.2 % fabrication loss).

Table 3 summarizes the total of eight fuel-cycle cases analyzed in this paper. These cases are based on the possible combinations of short (365.25 EFPD) versus long (547.875 EFPD) SFR cycle lengths, Pu-only recycling versus TRU recycling, and Type-a versus Type-b mass-flow paths. The Pu production rate of the SFR core can be relatively easily controlled without significantly varying the core inventory by changing the size of the axial blanket without rearranging the driver/blanket assemblies and batch sizes. Thus, the study is performed by increasing the size of axial blanket located at the top and bottom of the reference SFR core. (Note that the reference core model has 40 cm (20 cm top + 20 cm bottom) of axial blanket.) While the variation of the axial blanket size is the preferable option, increasing the axial size of the core could result in the increase of the sodium void coefficient by reducing axial neutron leakage. However, this study focuses more on the fuel-cycle performance, and at the end of the study the size of the axial blanket will be translated into SFR design flexibility in each fuel-cycle case. By combining with PWR calculation results, the size of the axial blanket is determined so that the unused amount of Pu/TRU, U_n in Eq. (1), turns out to be close to zero every year.

Table 3. Analyzed fuel-cycle cases and corresponding reactor models and type of fuel cycles.

Fuel cycle cases	Type of fuel cycle	Type of SFR	Type of PWR-MOX
FC-Pu-short-a	a	Pu-short-a	Pu-a
FC-Pu-short-b	b	Pu-short-b	Pu-b
FC-Pu-long-a	a	Pu-long-a	Pu-a
FC-Pu-long-b	b	Pu-long-b	Pu-b
FC-TRU-short-a	a	TRU-short-a	TRU-a
FC-TRU-short-b	b	TRU-short-b	TRU-b
FC-TRU-long-a	a	TRU-long-a	TRU-a
FC-TRU-long-b	b	TRU-long-b	TRU-b

Table 4 presents calculated core performances and mass-flows of SFR stages for the Pu-only recycling cases, and Table 5 shows those for the PWR stages. The same set of results for TRU recycling cases are shown in Tables 6 and 7. As seen in these tables, while slightly lower Pu/TRU inventories are required for SFRs in the Type-a scenario due to higher fissile quality in their charged fuels, Pu/TRU inventories of PWRs in the Type-a scenario are more than twice the inventories of PWRs in the Type-b scenario since PWRs in the Type-a scenario recycles their own Pu so that their fuels have high Pu/TRU content because of low fissile quality. As a result, in order to cover the Pu/TRU inventories of additional fleets in the Type-a scenario for 1% annual growth, a taller axial blanket is needed in order to breed more Pu/TRU. SFRs in the Type-b scenario, on the other hand, require much shorter axial blankets than those in the Type-a scenario, almost the same size as that of the reference core (40 cm). In this regard, SFRs in the Type-b scenario have more design flexibility than those in the Type-a scenario. The only concern in the Type-b scenario is the higher Pu content in SFR fuel than that of Type-a. It can also be observed that increasing the batch size of the SFR core while shortening the cycle length can reduce the Pu/TRU inventory requirement (short-a and short-b cases) so that the size of axial blanket can be shortened. However, discharge fast fluence reaches the limit of HT-9 cladding (4.0×10^{23} n/cm^2).

Table 4. Core performances and mass-flows of SFR stages for Pu-only recycling cases.

Type of SFR	Pu-short-a	Pu-short-b	Pu-long-a	Pu-long-b
Axial blanket size [cm]	60	37	65	41
Average discharge burnup [GWd/t]	25.0	28.9	28.2	32.8
Peak discharge fast fluence [10^{23} n/cm^2]	4.0	4.0	3.7	3.7
Number of batches	5		3 (driver & inner blanket) 5 (outer blanket)	
Fresh fuel Pu content [wt%]	22.0	26.3	21.9	26.1
Cycle length [EFPD]	365.3	365.3	547.9	547.9
Peak power density [W/cm^3]	343.4	346.5	342.2	344.1
BOEC Pu core inventory* [t/GWe]	5.719	6.519	5.885	6.713
Pu charge rate* [t/GWe-EFPY]	1.001	1.192	1.105	1.318
Pu discharge rate* [t/GWe-EFPY]	1.328	1.437	1.441	1.572
MA discharge rate* [t/GWe-EFPY]	0.018	0.037	0.018	0.040
Excess amount of Pu [t/GWe-EFPY]	0.144	0.122	0.152	0.130

*The mass necessary to produce 70 % of total energy.

Table 5. Core performances and mass-flow of PWR stages for Pu-only recycling cases.

Type of PWR-MOX	Pu-a	Pu-b
Average discharge burnup [GWd/t]	50.0	50.0
Fresh fuel Pu content [wt%]	9.12	4.15
Cycle length [EFPD]	471.4	471.4
Specific power [W/g]	35.36	35.36
Initial core Pu inventory* [t/GWe]	1.786	0.776
Pu charge rate* [t/GWe-EFPY]	0.601	0.275
Pu discharge rate* [t/GWe-EFPY]	0.439	0.171
MA discharge rate* [t/GWe-EFPY]	0.048	0.014

*The mass necessary to produce 30 % of total energy.

Table 6. Core performances and mass-flow of SFR stages for TRU recycling cases.

Type of SFR	TRU-short-a	TRU-short-b	TRU-long-a	TRU-long-b
Axial blanket size [cm]	56	35	63	39
Average discharge burnup [GWd/t]	25.6	29.3	28.6	33.2
Peak discharge fast fluence [10^{23} n/cm^2]	4.0	4.0	3.7	3.7
Number of batches	5		3 (driver & inner blanket) 5 (outer blanket)	
Fresh fuel TRU content [wt%]	25.8	28.5	25.7	28.4
Cycle length [EFPD]	365.3	365.3	547.9	547.9
Peak power density [W/cm^3]	346.9	349.1	344.7	345.9
BOEC TRU core inventory* [t/GWe]	6.526	7.046	6.719	7.231
TRU charge rate* [t/GWe-EFPY]	1.175	1.300	1.302	1.437
TRU discharge rate* [t/GWe-EFPY]	1.472	1.545	1.610	1.693
MA discharge rate* [t/GWe-EFPY]	0.132	0.116	0.149	0.130
Excess amount of TRU [t/GWe-EFPY]	0.154	0.135	0.164	0.143

*The mass necessary to produce 70 % of total energy.

Table 7. Core performances and mass-flow of PWR stages for TRU recycling cases.

Type of PWR-MOX	TRU-a	TRU-b
Average discharge burnup [GWd/t]	50.0	50.0
Fresh fuel TRU content [wt%]	9.12	4.10
Cycle length [EFPD]	471.4	471.4
Specific power [W/g]	35.36	35.36
Initial core TRU inventory* [t/GWe]	1.837	0.772
TRU charge rate* [t/GWe-EFPY]	0.606	0.273
TRU discharge rate* [t/GWe-EFPY]	0.486	0.183
MA discharge rate* [t/GWe-EFPY]	0.048	0.014

*The mass necessary to produce 30 % of total energy.

Table 8 shows the total amount of disposed waste from each fuel cycle case, along with its MA content. TRU recycling cases generally produce lower amounts of waste, as well as lower amounts of MA in the waste, than Pu-only recycling cases because most of the TRU is recycled and remains within closed fuel-cycle paths. By comparing Types-a and b scenarios, Type-a produces slightly larger amounts of waste than Type-b since the SFR core per unit energy in the Type-a scenario is larger than that of Type-b, therefore it discharges a larger amount of heavy metal, in which small portion is lost during reprocessing and goes to waste disposal (1.2% in this analysis). By looking at Pu-only recycling cases, disposed waste from the Type-b scenario contains less MA than the Type-a scenario. This is primarily caused by much smaller amounts of MA discharged from Type-b PWR-MOX than Type-a because of lower Pu content in the fuel which is transmuted into MA during irradiation. In this respect, the Type-b scenario has a capable of reducing the MA content in the disposed waste even with Pu-only recycling.

Table 8. Total amount of disposed waste and its MA content.

Fuel cycle cases	Total amount of disposed waste [t/GWe-EFPY]	MA in disposed waste [t/GWe-EFPY]
FC-Pu-short-a	1.426	0.065
FC-Pu-short-b	1.371	0.052
FC-Pu-long-a	1.391	0.066
FC-Pu-long-b	1.342	0.054
FC-TRU-short-a	1.355	0.002
FC-TRU-short-b	1.316	0.002
FC-TRU-long-a	1.324	0.002
FC-TRU-long-b	1.286	0.002

Figures 4-7 compare radioactivity, decay heat, ingestion and inhalation radiotoxicities, respectively, of disposed waste from each fuel-cycle case over the time span from 0 to 10^6 years. For clarity, a log-scale is used in both axes. As expected, all presented data for TRU recycling cases are lower than those of Pu-only recycling cases by eliminating significant contributions from key MAs such as ^{241}Am and ^{244}Cm. Among TRU recycling cases, there is no clear visual difference between Type-a and Type-b scenarios since there is no significant difference in MA content in disposed waste, except for the inhalation radiotoxicity, which is quite sensitive to the MA content compared to other three data. On the other hand, by comparing the Pu-only recycling cases, although it is not as effective as TRU recycling, it can be observed that there is a significant reduction in presented data for the Type-b scenario, in particular for inhalation radiotoxicity which is approximately a half of the Type-a scenario initially. Therefore, the Type-b scenario has clear advantages in Pu-only recycling in terms of SFR design flexibility and MA reduction in the disposed waste.

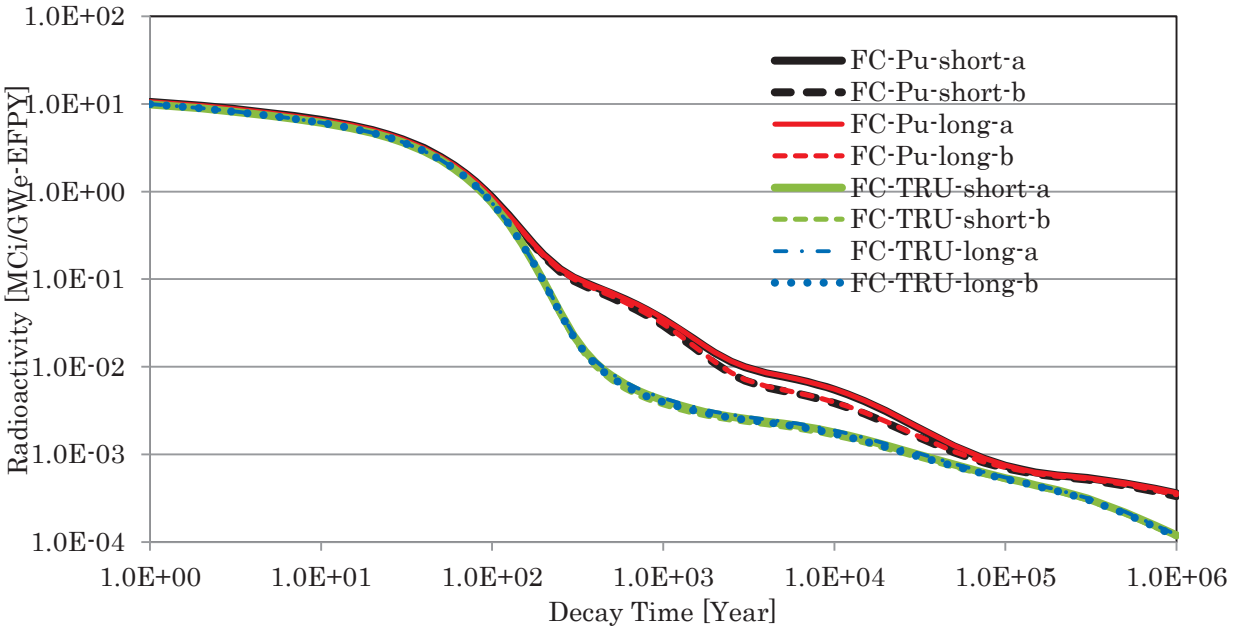

Figure 4. Radioactivity of disposed waste in each fuel-cycle case.

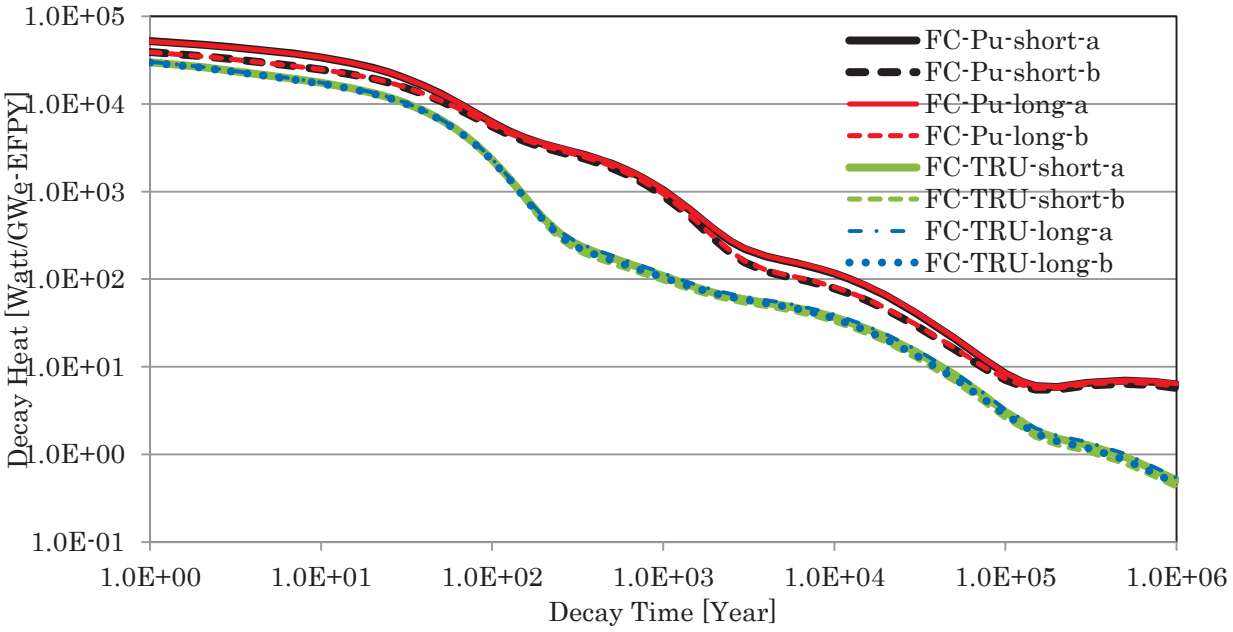

Figure 5. Decay heat of disposed waste in each fuel-cycle case.

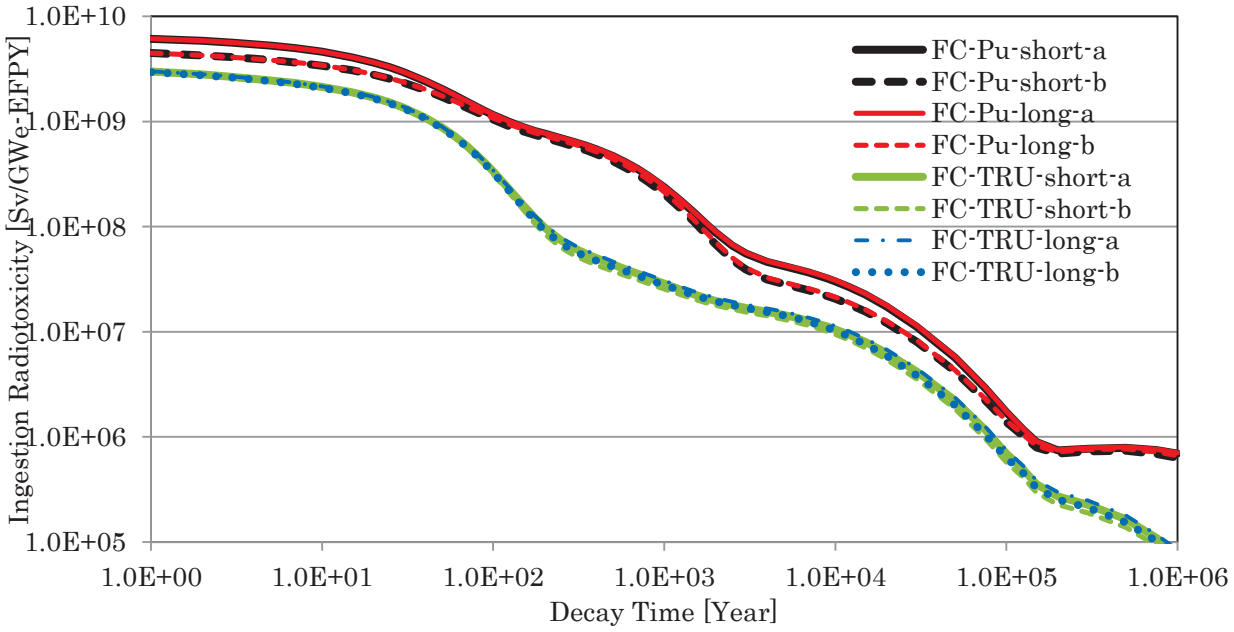

Figure 6. Ingestion radiotoxicity of disposed waste in each fuel-cycle case.

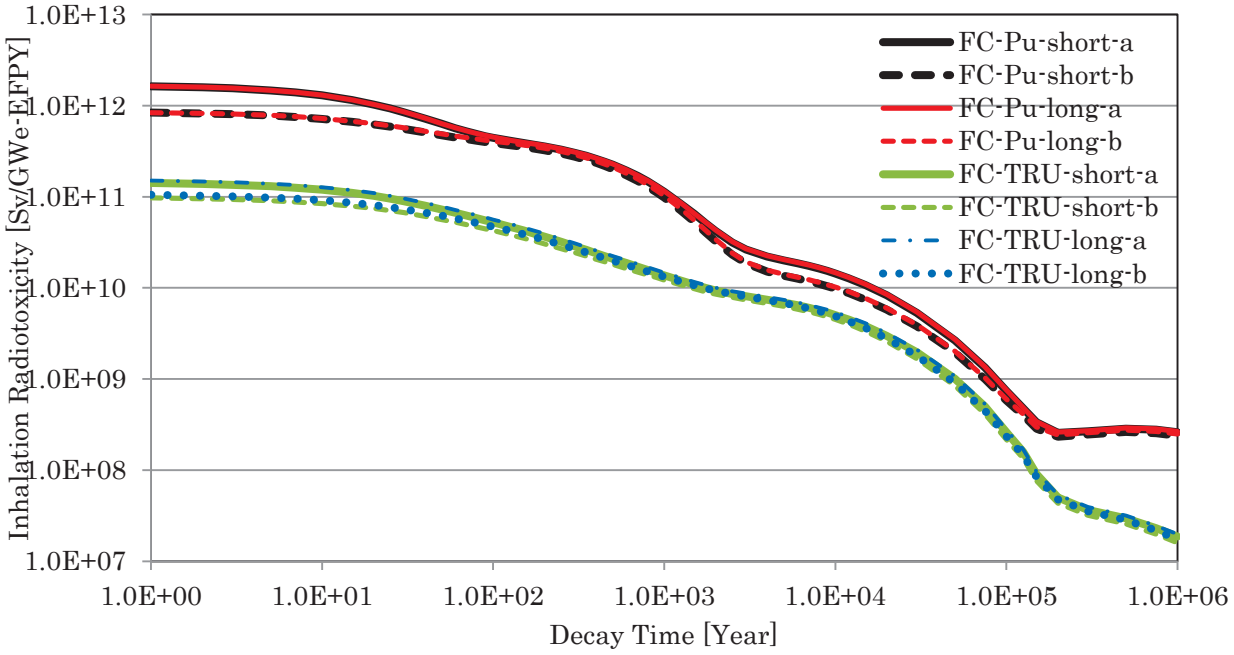

Figure 7. Inhalation radiotoxicity of disposed waste in each fuel-cycle case.

5. CONCLUSIONS

In this paper, the impact of modifications in closed fuel-cycle scenarios consisting of SFR and PWR-MOX systems on SFR core design, mass-flow and waste characterization was investigated. The study was performed by introducing a total of eight fuel-cycle cases that slightly differed in their fuel-cycle scenarios, core designs, and types of heavy metals recycled (Pu or TRU). The major exchange in the fuel-cycle scenarios considered here was imposed in the PWR-MOX stage such that one set of cases recycled discharged Pu/TRU and fabricated MOX fuel by topping Pu/TRU recovered from the SFR blanket (Type-a scenario), and the other used only recovered Pu/TRU from the SFR blanket, and its discharged Pu/TRU was sent to SFR metallic fuel fabrication (Type-b scenario). All analyses performed in this paper also took into account 1% of annual growth in electric power production and 1.2 % total recycling losses. Therefore, the size of axial blanket in SFR reactor cores was adjusted to produce the extra amount of Pu/TRU for covering losses and the additional reactors built for the 1% growth in each year.

The study showed that the Type-b scenario was capable of reducing the amount of MA content in the disposed waste even in Pu-only recycling systems primarily by reducing the amount of MA produced from PWR-MOX. It was also shown that the Type-b scenario was able to cover 1% annual electric production growth with much smaller size of axial blankets in SFR cores than SFR cores in the Type-a scenario. In this regard, SFRs in the Type-b scenario could have more design flexibility than those in the Type-a scenario. The only concern in the Type-b scenario was the higher Pu content in SFR fuel than that of Type-a. However, this could be remedied by rearranging driver and blanket assembly configurations. Note that in this study only limited variations in reactor designs were made. More robust changes in reactor designs could optimize the results and emphasize the effectiveness of the Type-b scenario.

ACKNOWLEDGMENTS

This work was supported by U. S. Department of Energy under contract DE-AC07-05ID14517.

REFERENCES

[1] T. Kim, T. Taiwo, and R. Wigeland, “Summary of FY 2014 Tradeoff Study in Fuel Cycle Performance,” FCRD-FCO-2015-000171 (2015).
[2] R. Wigeland, et al., “Nuclear Fuel Cycle Evaluation and Screening – Final Report,” INL/EXT-14-31465 (2014).
[3] A. E. Dubberley, K. Yoshida, C. E. Boardman, and T. Wu, “SuperPRISM Oxide and Metal Fuel Core Designs,” *Proc. 8th Int. Conf. on Nucl. Eng. (ICONE 8)*, April 2-6, 2000, Baltimore, MD, USA (2000).
[4] B. J. Toppel, “The Fuel Cycle Analysis Capability REBUS-3,” ANL-83-2 (1983).
[5] R. D. Lawrence, “The DIF3D Nodal Neutronic Option for Two- and Three-Dimensional Diffusion Theory Calculations in Hexagonal Geometry,” ANL-93-1 (1983).
[6] C. H. Lee and W. S. Yang, “MC^2-3: Multigroup Cross Section Generation Code for Fast Reac-

tor Analysis," ANL/NE-11-41 Rev.1 (2012).
[7] *Scale: A Comprehensive Modeling and Simulation Suite for Nuclear Safety Analysis and Design*, ORNL/TM-2005/39, Version 6.1, June 2011. Available from Radiation Safety Information Computational Center at Oak Ridge National Laboratory as CCC-785.
[8] R. G. Cochran and N. Tsoulfanidis, The Nuclear Fuel Cycle: Analysis and Management, American Nuclear Society, La Grange Park, IL (1990).
[9] I. C. Gauld, "ORIGEN-S: Depletion Module to Calculate Neutron Activation, Actinide Transmutation, Fission Product Generation, and Radiation Source Terms," ORNL/TM-2005/39, Version 6.1, Sect. F7 (June 2011).
[10] A. G. Croff, "ORIGEN2: A Versatile Computer Code for Calculating the Nuclide Compositions and Characteristics of Nuclear Materials," *Nucl. Technol*., **62**, 335-351 (1983).
[11] ICRP, 2012. Compendium of Dose Coefficients based on ICRP Publication 60. ICRP Publication 119. Ann. ICRP 41 (Suppl.).